Efficient prediction of aeroelastic behaviour including geometric non-linearities

M. Y. Harmin, J.E. Cooper
University of Liverpool, School of Engineering,
L69 3GH, Liverpool, England, United Kingdom
e-mail: **m.harmin@liverpool.ac.uk**
j.e.cooper@liverpool.ac.uk

Abstract
A procedure for developing efficient aeroelastic Reduced Order Models (ROMs) for aerospace structures containing geometric non-linearities is described. The structural modelling is based upon a combined modal/ Finite Element approach that describes the non-linear stiffening effects from results of non-linear static analyses for a range of prescribed inputs. Once the structural ROM has been defined, it is coupled to the aerodynamic model. The aeroelastic model can then be used to predict the dynamic aeroelastic behaviour of the defined structure. The methodology is demonstrated on the aeroelastic model of a flexible high-aspect ratio wing.

Nomenclature

$\mathbb{A},\mathbb{E}$	=	structural physical mass/stiffness	ρ	=	air density
$\boldsymbol{A}, \boldsymbol{E}$	=	structural modal mass/stiffness	a_w	=	lift curve slope
$\mathbb{F}$	=	physical force vector	$M_{\dot{\theta}}$	=	Non dimensional pitch damping
$\boldsymbol{f}$	=	modal force vector	s	=	half wing span
$r(x,t)$	=	physical displacement vector	c	=	chord
$p(t)$	=	modal displacement vector	b	=	semi-1chord
$\phi(x)$	=	eigenvectors	V	=	velocity
N	=	Number of DOF in FE model	L	=	Lift
NR	=	Number of DOF in reduced modal model	M	=	Pitching moment
			$\boldsymbol{AIC}$	=	Aerodynamic influence matrix
NT	=	Number of nonlinear static test cases	k	=	reduced frequency
			q	=	dynamic air pressure
NA	=	Number of nonlinear stiffness coefficients	A_n	=	Roger matrices
			β_n	=	Aerodynamic lag parameters
NL	=	Number of aerodynamic lag parameters			
$\boldsymbol{\mathcal{A}_r}$	=	Nonlinear stiffness coefficients			
H	=	Contribution factor			
$R_T{}^2$	=	Cumulative goodness of fit			

1 Introduction

There has been a growth of interest in the development of highly flexible UAV aircraft. Perhaps the best known instance is the Helios aircraft that failed during a flight in 2003 due to the response to a gust. One of the causes of the accident found by the investigation that followed was the lack of appropriate analyses for highly flexible aerospace structures [1] leading to inappropriate decisions to fly a certain configuration. One characteristic of such aircraft is that the structural stiffness behaves in a non-linear manner due to geometric stiffening or softening, and consequently the conventional approach to aeroelastic analysis is not valid. The geometric non-linear effects of such large structures can also have a dramatic effect upon the flight dynamics; Palacios et al. [2] reviewed the most important aspects of high aspect ratio aircraft affected by the non-linear structure, including longitudinal stability, body-freedom flutter and gust response (and subsequent loads). They emphasised the need for computationally efficient reduced order time domain simulations to predict the coupled aeroelastic/flight dynamic interactions. The effect of geometric non-linearities is not solely confined to HALE (High Altitude Long Endurance) aircraft and the current generation of large commercial and military aircraft exhibit some of the above characteristics. Although there has been a great deal of research devoted to the effect of non-linearities on aeroelastic behaviour, this has primarily been directed towards aerodynamic non-linearities in the transonic flight regime, or structural nonlinearities such as freeplay and hysteresis occurring on control surfaces. Most of the work [2-8] directed at modeling the geometric stiffening characteristics for aeroelastic models of HALE type aircraft has employed equivalent non-linear beam models.

There have been a number of approaches developed to use commercial Finite Element software to enable the development of Reduced Order structural models. In particular the Modal/FE approach of McEwan et al. [9, 10] performs a static analysis for a number of defined prescribed loading cases. These displacements are then curve fitted using a regression analysis in order to define non-linear stiffness terms that can be added to the conventional modal model. A similar approach is used in the ELSTEP methodology [11, 12] which applies prescribed displacements. Once the reduced order model is produced it is then very efficient to run time domain simulations for a large number of design cases. The Modal / Finite Element (FE) approach has been used very successfully [10, 13] for the prediction of response of aircraft panels subjected to large acoustic excitations. A recent application of the ELSTEP approach has been to combine it [14, 15] to hypersonic aerodynamic models in order to produce efficient coupled non-linear aeroelastic models of membrane type structures.

In this paper, a combined modal/finite element approach of McEwan et al. [9, 10] is implemented to model the geometric nonlinearities of studied structure, where Patil and Hodge's HALE wing model has been taken as an exemplar for this study. The prescribed load cases and resultant displacements from the static nonlinear test cases are transformed into the modal coordinates using the modal transformation of underlying linear mode system. The regression analysis is then performed to curve-fit on sets of nonlinear stiffness forces information in order to find the unknown nonlinear modal stiffness coefficients. Having obtained the nonlinear modal model, the aeroelastic analysis is then performed by coupling it with the aerodynamic model. Two different types of aerodynamic models have been considered in this study, which are (1) modified aerodynamic strip theory, and (2) a Rational Function Approximation (RFA) of doublet lattice by using the Roger procedure.

2 Formulation

2.1 Combined modal/finite element approach [9, 10]

2.1.1 Nonlinear structure modal model

The equations of motion of dynamic system in physical space including stiffness nonlinearity can be represented as

$$\mathbb{A}\ddot{r} + \alpha\mathbb{A}\dot{r} + \mathbb{E}_{\mathbf{L}}r + \{\mathbb{E}_{\mathbf{NL}}(r)\} = \{\mathbb{F}\} \tag{1}$$

where $\mathbb{A}$ is the N×N assembled mass matrix, $\mathbb{E}_L$ is the N×N assembled linear stiffness matrix, $\mathbb{E}_{NL}$(r) is the N×1 vector of nonlinear stiffness function, $\mathbb{F}$ is the N×1 vector of applied nodal forces, α is the proportional mass damping coefficient, and r(t) is the N×1 vector of spatial displacements. The transformation between the physical space and modal space is performed using the modal transformation

$$r(x,t) = \phi(x)p(t) \tag{2}$$

where $p(t)$ is the NR×1 vector of time-dependent generalized modal coordinates and $\phi(x)$ is the N×NR matrix of the underlying linear mode shapes. The number of degrees of freedom in the modal model can be reduced (NR<<N) depending on the frequency range or modes of interest. Substituting the modal transformation of equation (2) into equation (1) and pre-multiplying by $[\phi]^T$ yields

$$\phi^T\mathbb{A}\phi\ddot{p} + \alpha\phi^T\mathbb{A}\phi\dot{p} + \phi^T\mathbb{E}_{\mathbf{L}}\phi p + \phi^T\{\mathbb{E}_{\mathbf{NL}}(r)\}\phi p = \phi^T\{\mathbb{F}\} \tag{3}$$

Here, a set of coupled physical systems are modified into a set of uncoupled single DOF modal systems by using the orthogonality of the modes. Therefore, the equations of motion in modal coordinates become

$$\boldsymbol{A}\ddot{p} + \alpha\boldsymbol{A}\dot{p} + \boldsymbol{E_L}p + \{\boldsymbol{E_{NL}}(p)\} = \{\boldsymbol{f}\} \tag{4}$$

where matrix $\boldsymbol{A}$ and $\boldsymbol{E_L}$ are now diagonal matrices of size NR×NR. However, it should be noted that the nonlinear modal stiffness matrix $\{\boldsymbol{E_{NL}}(p)\}$ which is a NR×1 vector, may contain cross-coupling terms and is a function of modal coordinate, *p(t)*.

2.1.2 Strategy for generating static nonlinear finite element test cases

The implementation of the combined modal/Finite Element (FE) approach is based on nodal deflections obtained from a number of prescribed static non-linear load cases. Thus, when a static system is considered, the equations of motion which are given by equation (4) reduce to

$$\boldsymbol{E_L}p + \{\boldsymbol{E_{NL}}(p)\} = \{\boldsymbol{f}\} \tag{5}$$

and by rearranging the above equation, the nonlinear stiffness restoring forces can be written as

$$\{\boldsymbol{f}\} - \boldsymbol{E_L}\mathrm{p} = \{\boldsymbol{E_{NL}}(p)\} \tag{6}$$

A set of finite element nonlinear static test cases have to be defined by prescribing a set of applied loads in the finite element nodal space. The nonlinear modal stiffness coefficients are identified by performing

regression analysis on sets of information obtained from several nonlinear static test cases which have been transformed into the modal coordinates. These load cases can be generated by using the following equation:

$$\{\mathbb{F}\} = a_r\left(\frac{2i}{g-1}-1\right)\{\phi\}_r + a_s\left(\frac{2j}{g-1}-1\right)\{\phi\}_s \quad (7)$$

i = 0,1,.. g-1
j = 0,1,.. g-1

Here, a_r and a_s are the scalar weighting factors. The grid density value, g, is used to define the intermediate load cases and the eigenvectors {φ} can be obtained from 'normal mode analysis' by using any proprietary finite element software package.

The Patil and Hodges HALE wing model [4,16] has been taken as an example in this work. In order to define the geometric nonlinearities of the structure, the first three fundamental bending modes and the first torsion mode have been considered.

The structural bending nonlinearities are developed based on the simultaneous coupling of these bending modes only. With g taken as 2 for the bending case, this leads to a total of 19 test cases which can be derived using the equation (7). Due to the unknown characteristics of the stiffness nonlinearities, it has to be assumed that the nonlinear cross-couplings between these bending modes have significant effect on overall static and dynamic responses where a solution of certain modes may induce a response of other modes as well. Figure (1) shows the spatial distribution of the first three bending modes of the wing.

Before further implementation of this approach is made, the characteristics of the stiffness nonlinearities due to the bending of the structure need to be identified. Thus, by using any proprietary FE software package of nonlinear static analysis, the structure is analyzed with uniform incremental forces along the structure. Figure (2) shows the resultant deflections at the tip of the wing from this analysis. It is clearly shown that the structure experiences a stiffness hardening effect where the 'stiffening' behaviour occurs as the tip of the wing is deflected above than 1.5m.

Consequently, all of the defined 19 test cases must have minimum tip deflections greater than 1.5m. Therefore, care has to be taken when defining the scalar weighting factor so that no physical displacement of any of the test load cases will ever exceed these conditions. To ensure that all of the load cases are able to deflect the structure into the nonlinear region, comparisons are made between the resultant nodal displacements of linear static and nonlinear static solution as shown in figure (3).

For the structural nonlinearities due to torsion, the above procedure is repeated. The load cases are derived similarly as before using equation (7) with g taken as four. This leads to a total of seven load cases. Figure (4) shows the comparisons between the linear and nonlinear static FE solution in terms of torsional on the middle section of the wing model. It should be noted that the cross couplings between the bending modes and the torsion mode have not been considered in this paper; nevertheless, further work considering this effect is ongoing.

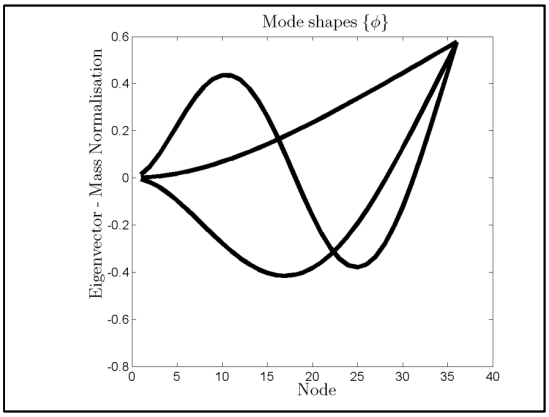

Figure (1) : First three bending mode shapes of considered model

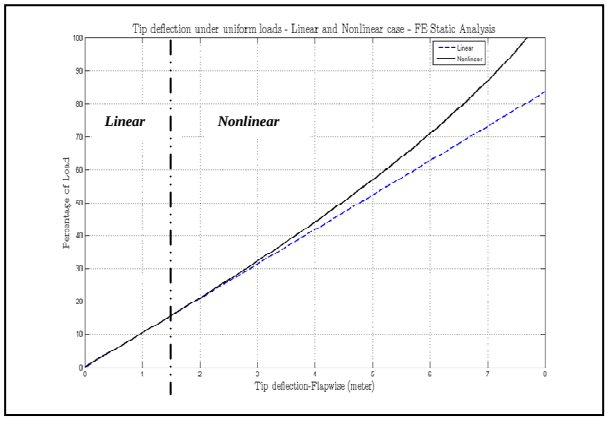

Figure (2) : Wing tip Nonlinear Deflection (NASTRAN static nonlinear analysis)

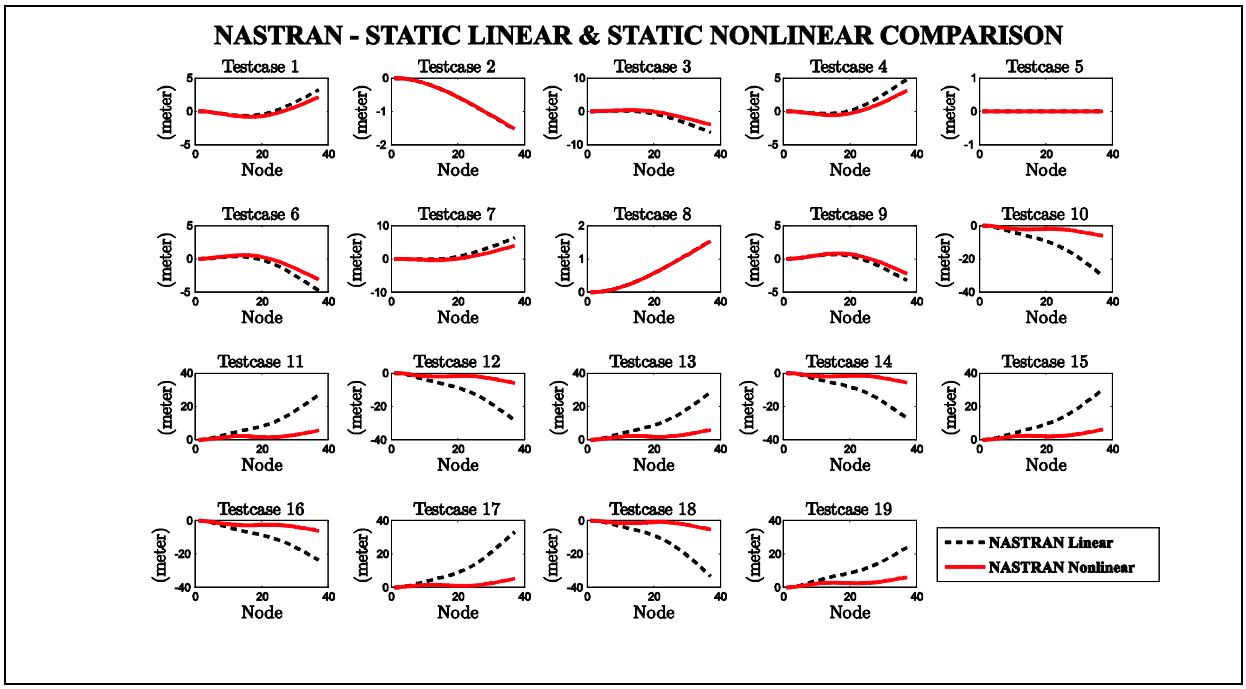

Figure (3) : displacement (bending) of Nastran-Linear Static and Nonlinear Static Solution

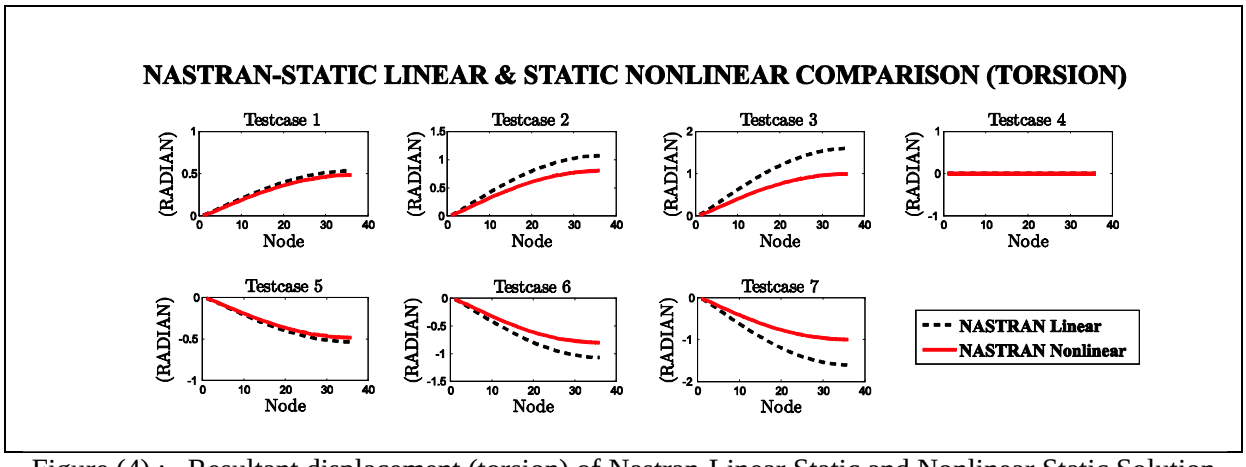

Figure (4) : Resultant displacement (torsion) of Nastran-Linear Static and Nonlinear Static Solution

Having defined the load cases, the static nonlinear finite element test cases can then be solved by using finite element software to obtain the resultant displacement for each of the test cases. Following this, the acquired information on the nodal forces and nodal displacements are then transformed into the modal space.

The transformation of nodal displacement into modal space can be calculated from the solution

$$\phi p = \mathrm{r} \tag{8}$$

while the applied modal force vector is obtained as

$$\boldsymbol{f} = \phi^T \mathbb{F} \tag{9}$$

2.1.3 Regression analysis, Curve fitting

An ordinary polynomial approach has been considered in order to curve fit the nonlinear forces. In this work, simultaneous coupling of up to two modes has been considered. From other studies made by the authors, it is found that the simultaneous couplings of more than two modes for the considered structure are very weak and can be safely neglected. Therefore, the polynomial of the nonlinear restoring forces will be derived as the following series of up to third order for some mode r

$$\boldsymbol{E_{NL(r)}}(p_1, p_2 \ldots p_{NR}) = \sum_{s=1}^{NR} \sum_{i=2}^{3} \boldsymbol{\mathcal{A}}_r \; p_s^i + \sum_{s=1}^{NR-1} \sum_{s+1}^{NR} \sum_{i=1}^{2} \sum_{j=1}^{3-i} \boldsymbol{\mathcal{A}}_r \; p_s^i \, p_t^j \tag{10}$$

Upon completion of the static nonlinear test cases, and with the acquired data of load-displacement in modal space, the nonlinear restoring force for each of the test cases can now be fitted to find the unknown nonlinear modal stiffness coefficients in a least squares sense. The nonlinear restoring forces for a certain mode r can now be shown in matrix form to be

$$\begin{Bmatrix} f_{r(1)} - \boldsymbol{E_{L(r)}} p_{r(1)} \\ f_{r(2)} - \boldsymbol{E_{L(r)}} p_{r(2)} \\ \vdots \\ \vdots \\ f_{r(NT)} - \boldsymbol{E_{L(r)}} p_{r(NT)} \end{Bmatrix} = \begin{bmatrix} \mathrm{p}^2_{1(1)} & \mathrm{p}^3_{1(1)} \; \ldots\ldots \\ \mathrm{p}^2_{1(2)} & \mathrm{p}^3_{1(2)} \; \ldots\ldots \\ \vdots & \vdots \\ \vdots & \vdots \\ \mathrm{p}^2_{1(\mathrm{NT})} & \mathrm{p}^3_{1(\mathrm{NT})} \; \ldots\ldots \end{bmatrix} \begin{Bmatrix} \boldsymbol{\mathcal{A}}_{r\,(1)} \\ \boldsymbol{\mathcal{A}}_{r\,(2)} \\ \vdots \\ \vdots \\ \boldsymbol{\mathcal{A}}_{r\,(NA)} \end{Bmatrix} \tag{11}$$

or represented as

$$\{f_r\}_{NL} \approx \{\widehat{f_r}\}_{NL} = [D_r]\{\boldsymbol{\mathcal{A}}_r\} \tag{12}$$

Here, $\{\widehat{f_r}\}_{NL}$ is a NT×1 vector of fitted values of nonlinear modal stiffness restoring forces, $[D_r]$ is NT×NA design matrix and $\{\boldsymbol{\mathcal{A}}_r\}$ is NA×1 vector containing the unknown values of nonlinear stiffness coefficients where both of these matrices are developed based on equation (10).

The Singular Value Decomposition (SVD) technique is implemented in order to find fitted values of the nonlinear stiffness coefficient $\{\boldsymbol{\mathcal{A}}_r\}$. This technique is able to solve the pseudo-inverse of a rectangular matrix that is suspected to be ill-conditioned. Here, the design matrix $[D_r]$ can be represented as

$$[D_r] = [U][W][V]^T \tag{13}$$

where [U] is a NT×NA matrix and $[V]^T$ is a NA×NA matrix. Both of these matrices are in orthogonal form, while [W] is NA×NA diagonal matrix consisting of positive real values of singular values.

$$\{\hat{f}_r\}_{NL} = [U][W][V]^T\{\boldsymbol{\mathcal{A}_r}\} \tag{14}$$

If $[D_r]^T[D_r]$ is a non-singular matrix, the nonlinear stiffness coefficients are found from

$$\{\boldsymbol{\mathcal{A}_r}\} = [V][W]^{-1}[U]^T\{\hat{f}_r\}_{NL} \tag{15}$$

If $[D_r]^T[D_r]$ is a singular matrix, then the $[W]^{-1}$ matrix will be partitioned to remove the non-contributing components such that

$$[W]^{-1} = \begin{cases} \frac{1}{\sigma_i} & if\ \sigma_i > tol \quad (small\ threshold) \\ 0 & otherwise \end{cases} \tag{16}$$

and the nonlinear stiffness coefficient can then be found by substituting the altered $[W]^{-1}$ into equation (15).

In order to obtain the appropriate combinations of the nonlinear polynomial terms, the backward elimination approach will be used to remove the redundant terms that give less significance to the overall solution. The contribution of each of the polynomial series in $[D_r]$ matrix can be found by solving the root mean square values (RMS) for each of the polynomial term, given as

$$H(j) = \sqrt{\frac{1}{NT}\sum_{i=1}^{NT}(D_r(i,j)\boldsymbol{\mathcal{A}_r}(j))^2} \tag{17}$$

The cumulative goodness of fit parameter, R_T^2, will be used as an objective function for terminating the backward elimination process.

$$R_T{}^2 = 1 - \frac{\left(\{\hat{f}_r\}_{NL} - [D_r]\{\boldsymbol{\mathcal{A}_r}\}\right)^T\left(\{\hat{f}_r\}_{NL} - [D_r]\{\boldsymbol{\mathcal{A}_r}\}\right)}{\{\hat{f}_r\}_{NL}^T\{\hat{f}_r\}_{NL}} \tag{18}$$

The threshold value of R_T is defined at a value close to one. The closer the R_T value to unity, the more polynomial terms will be retained in the series. A lower value of R_T will lead to a fewer terms; however, this may cause the model to become less accurate if too many terms are taken away from the polynomial series.

2.1.4 Verification

In order to verify the accuracy of the estimated nonlinear reduced order modal model (NLROMM), the following procedures was implemented. The modal force is first defined and the NLROMM solved using a Newton-Raphson approach in order to compute the modal displacements of the solution. The modal

displacements are then transformed into physical space and comparisons made with the finite element nonlinear static analysis. Once close agreement between the NLROMM and finite element analysis (FEA) is achieved, the NLROMM is suitable to be considered for further analysis.

2.2 Dynamic Aeroelastic Model

The general form of the aeroelastic analysis is developed by coupling the aerodynamic panels and the FE representations of the considered model [17]. When applied to dynamic systems, the dynamic behaviour of FE model relates the displacement and acceleration vectors to the force vector via the overall stiffness and mass matrices such that

$$R = \mathbb{A}\ddot{r} + \mathbb{E}r \tag{19}$$

This equation will be coupled with the aerodynamic model of lift and pitching moments to form the dynamic aeroelastic equation as

$$\mathbb{A}\ddot{r} + \mathbb{E}r = L + M \tag{20}$$

2.2.1 Dynamic Aeroelastic analysis using the modified aerodynamic strip theory

In a modified unsteady aerodynamic strip theory (MAST) [17] approach, the wing is considered to be composed of a number of aerodynamic panels in which the lift acting on the quarter chord is assumed to be proportional to the dynamic pressure, local angle of attack, lift curve slope and the downwash due to vertical motion. Since the wing is modelled by a series of beam elements in the FEA, the equivalent forces and moments acting at the element nodes due to the aerodynamic forces on the quarter chord of the wing have to be determined. This can be done by considering the idea of 'kinematically equivalent nodal forces' where the nodal forces are assumed to do equivalent work as the work done under distributed load over the element. Figure (5) shows the equivalent forces and moments acting on the elemental nodes.

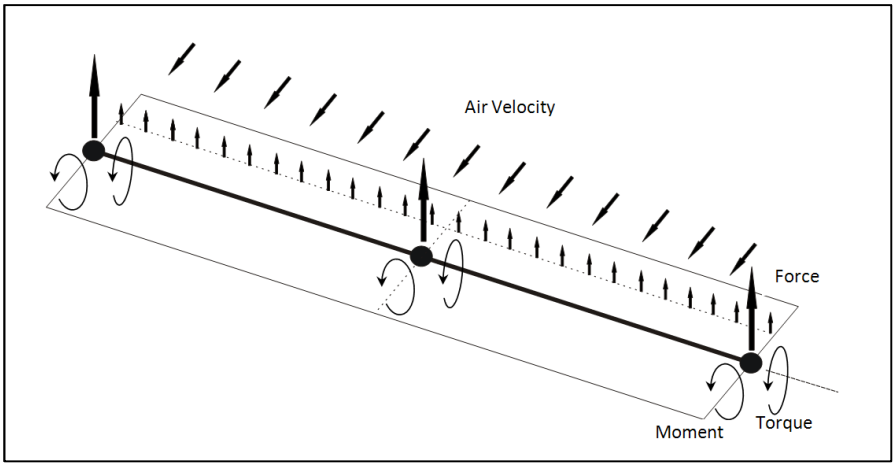

Figure (5) : Equivalent forces and moments at the beam nodes

The lift and pitching moment of an elemental streamwise strip on the wing can be represented as

$$L = \frac{\rho V^2}{2}\boldsymbol{T_1} a_w sc \boldsymbol{T_2}\left[r(\alpha + \alpha_o) + \dot{r}(\dot{z})\frac{1}{V}\right] \tag{21}$$

$$M = \frac{\rho V^2}{2}\boldsymbol{T_1} sc^2\left[e a_w \boldsymbol{T_2}\left[r(\alpha) + \frac{1}{V}\dot{r}(\dot{z})\right] + \frac{M_{\dot{\theta}} c}{4V}\boldsymbol{T_2}\dot{r}(\dot{\theta})\right] \tag{22}$$

where $\mathbf{T_1}$ is the transformation matrix that maps forces between the aerodynamic panels and the structural element model, and $\mathbf{T_2}$ is another transformation matrix that relates the physical coordinate to the acting forces and moments.Thus, from equation (20), the full aeroelastic equations may be written in terms of aerodynamic damping and stiffness as

$$\mathbb{A}\ddot{r} + \mathbb{E}r = \frac{\rho V^2}{2}\boldsymbol{AIC_d}\dot{r} + \frac{\rho V^2}{2}\boldsymbol{AIC_s}r \tag{23}$$

This set of equations can be transformed into the modal space using a similar modal transformation as in equation (2). This will allow the modal aeroelastic equations of motion to be combined together with the geometric nonlinear term that can be obtained using the *combined modal/FE* approach, such that

$$\boldsymbol{A}\ddot{q} + \mathbf{E_L}q + \mathbf{E_{NL}}(q) = \frac{\rho V^2}{2}\phi^t \boldsymbol{AIC_d}\phi\dot{q} + \frac{\rho V^2}{2}\phi^t \boldsymbol{AIC_s}\phi\{q + q_o\} \tag{24}$$

It should be noted that, in this study, the aeroelastic analysis is simulated in the modal space as the geometric nonlinearities of the structure using the *combined modal/FE* technique is obtained in this coordinates. The modal form of equation (24) can be solved using time domain integration to calculate the response for any given input force (initial deflection, initial velocity or gust).

2.2.2 Dynamic Aeroelastic analysis with the inclusion of frequency dependent aerodynamics

A better representation of the aerodynamic model compared to the MAST which has been described before will be used via Doublet Lattice Methods (DLM) in order to predict accurately the dependency of aerodynamic forces and moments on the frequency content of dynamic motions [17]. From equation (7), the full aeroelastic equation with the inclusion of frequency dependent aerodynamics may be written as

$$\mathbb{A}\ddot{r} + \mathbb{E}r = \frac{\rho V^2}{2}\frac{b}{k}\boldsymbol{AIC_d}\dot{r} + \frac{\rho V^2}{2}\boldsymbol{AIC_s}r \tag{25}$$

where AIC matrices in the above equation are in complex form and a function of reduced frequency

$$k = \frac{\omega b}{V} \tag{26}$$

The modal aeroelastic equations of motion with the inclusion of geometric nonlinearities can then be expressed as

$$\boldsymbol{A}\ddot{p} + \mathbf{E_L}p + \mathbf{E_{NL}}(p) = \frac{\rho V^2}{2}\frac{b}{k}\phi^t \boldsymbol{AIC_d}\phi\dot{p} + \frac{\rho V^2}{2}\phi^t \boldsymbol{AIC_s}\phi\{p + p_o\} = \boldsymbol{Q}_{aero} \tag{27}$$

where $\boldsymbol{Q}_{aero}$ is the generalised aerodynamic forces and is in a function of the reduced frequency.

In this work, results from the three-dimensional aerodynamic panel approach of DLM have been extracted from MSC NASTRAN-Aeroelastic Analysis by using the Direct Matrix Abstraction Program (DMAP). Here, the complex form of modal AIC matrices is obtained at a range of reduced frequencies for a given flight condition. A Roger procedure [18] is then employed to approximate the RFA of the AIC matrices and the state-space time domain may be formed. With this approach, the used of convolution time domain integral can be avoided. Thus, a much simple mathematical representation can be formed in solving the time domain integration.

Alternatively, the above equation can be transformed and written in term of Laplace domain as:

$$(\boldsymbol{A}s^2 + \mathbf{E_L})p(s) + \mathbf{E_{NL}}(p(s)) = \frac{\rho V^2}{2}\boldsymbol{Q}(s)p(s) \tag{28}$$

and the RFA of the generalised aerodynamic matrices $\boldsymbol{Q}(s)$ are written in the form

$$\boldsymbol{Q}(s) = A_0 + A_1\left(\frac{sb}{V}\right) + A_2\left(\frac{sb}{V}\right)^2 + \left(\frac{V}{b}\right)\sum_{n=1}^{N_L}\frac{A_{n+2}\ s}{\left(s + \left(\frac{V}{b}\right)\beta_n\right)} \tag{29}$$

Here, A_n is a NR×NR unknown matrix to be found and β_n are the aerodynamic lag parameters which can be calculated as [20]

$$\beta_i = -1.7k_{max}\frac{i}{(N_L+1)^2} \tag{30}$$

where k_{max} is the maximum reduced frequency at which the AIC matrices was obtained from the MSC NASTRAN-aeroelastic analysis, and N_L is the number of lag parameters. Recalling the definition of the reduced frequency and since the Laplace variable s = iω, thus the RFA of equation (29) can be written in terms of reduced frequency as

$$\boldsymbol{Q}(s) = A_0 + A_1(ik) + A_2(ik)^2 + \sum_{n=1}^{N_L}\frac{A_{n+2}\ ik}{(ik+\beta_n)} \tag{31}$$

The unknown A_n coefficients can be estimated by using the minimization procedure (method of least square) of sum of squares of errors between the RFA and AIC matrix as follows

$$\varepsilon_{rs} = \sum_{m=1}^{N_k}\left(Q_{rs}(ik_m) - AIC_{rs}(ik_m)\right)^2 \tag{32}$$

with the subscript 'rs' indicates the rsth element of each matrix. By differentiating equation (32) with respect to A_n and setting this gradient equals to zero such that

$$\left(\frac{\partial\varepsilon}{\partial A_n}\right)_{rs} = 0 \tag{33}$$

the following equation is then established

$$\begin{bmatrix} 1 & ik_1 & -k_1^2 & \frac{ik_1}{ik_1+\beta_1} & \dots & \frac{ik_1}{ik_1+\beta_{N_L}} \\ 1 & ik_2 & -k_2^2 & \frac{ik_2}{ik_2+\beta_1} & \dots & \frac{ik_2}{ik_2+\beta_{N_L}} \\ \vdots & \vdots & \vdots & \vdots & \vdots & \vdots \\ 1 & ik_{N_K} & -k_{N_K}^2 & \frac{ik_{N_K}}{ik_{N_K}+\beta_1} & \dots & \frac{ik_{N_K}}{ik_{N_k}+\beta_{N_L}} \end{bmatrix} \begin{Bmatrix} A_0 \\ A_1 \\ A_2 \\ A_3 \\ \vdots \\ A_{N_L+2} \end{Bmatrix}_{rs} = \begin{Bmatrix} AIC(ik_1) \\ AIC(ik_2) \\ AIC(ik_3) \\ AIC(ik_4) \\ \vdots \\ AIC(ik_{N_K}) \end{Bmatrix}_{rs} \tag{34}$$

In order to obtain the fitted value of the unknown A_n coefficients, the complex form of above notation is partitioned into the real and imaginary part. Then these can be solved using the least squares method. Thus, equation (34) may be rewritten as

$$\begin{bmatrix} \begin{bmatrix} 1 & 0 & -k_1^2 & \frac{k_1^2}{k_1^2+\beta_1^2} & \dots & \frac{k_1^2}{k_1^2+\beta_{N_L}^2} \\ \vdots & \vdots & \vdots & \vdots & & \vdots \\ 1 & 0 & -k_{N_K}^2 & \frac{k_{N_K}^2}{k_{N_K}^2+\beta_1^2} & \dots & \frac{k_{N_K}^2}{k_{N_K}^2+\beta_{N_L}^2} \end{bmatrix}_{real} \\ \begin{bmatrix} 0 & ik_1 & 0 & -\frac{k_1 p_1^2}{k_1^2+\beta_1^2} & \dots & -\frac{k_1\beta_{N_L}^2}{k_1^2+p_{N_L}^2} \\ \vdots & \vdots & \vdots & \vdots & & \vdots \\ 0 & ik_{N_K} & 0 & -\frac{k_{N_K}\beta_1^2}{k_{N_K}^2+\beta_1^2} & \dots & -\frac{k_{N_K}\beta_{N_L}^2}{k_{N_K}^2+\beta_{N_L}^2} \end{bmatrix}_{imag} \end{bmatrix} \begin{Bmatrix} A_0 \\ A_1 \\ A_2 \\ A_3 \\ \vdots \\ A_{N_L+2} \end{Bmatrix}_{rs} = \begin{Bmatrix} \begin{Bmatrix} AIC(k_1) \\ \vdots \\ AIC(k_{N_K}) \end{Bmatrix}_{real} \\ \begin{Bmatrix} AIC(k_1) \\ \vdots \\ AIC(k_{N_K}) \end{Bmatrix}_{imag} \end{Bmatrix}_{rs} \tag{35}$$

Having estimated the unknown A_{rs} values, the time domain models can be written as

$$\boldsymbol{A}\ddot{p} + \mathbf{E_L}p + \mathbf{E_{NL}}(p) = A_0 qp + \left(\frac{b}{V}\right) A_1 q\dot{p} + \left(\frac{b}{V}\right)^2 A_2 q\ddot{p} + q\sum_{n=1}^{N_L} A_n \dot{p}_{a_n} \tag{36}$$

where $q = \frac{\rho V^2}{2}$ is the dynamic pressure. Rearranging the above expression yields

$$\left(\boldsymbol{A} - \left(\frac{b}{V}\right)^2 A_2 q\right)\ddot{p} - \left(\frac{b}{V}\right) A_1 q\dot{p} + (\mathbf{E_L} - A_0 q)p = -\mathbf{E_{NL}}(p) + q\sum_{n=1}^{N_L} A_n \dot{p}_{a_n} \tag{37}$$

or in a shorthand notation

$$(\widetilde{\boldsymbol{A}})\ddot{p} + \widetilde{\boldsymbol{D}}\dot{p} + (\tilde{\mathbf{E}}_\mathbf{L})p = -\mathbf{E_{NL}}(p) + q\sum_{n=1}^{N_L} A_n \dot{p}_{a_n} \tag{38}$$

The augmented states which arise from the convolution integral of the inverse Laplace transform of the ***Q****(s)* matrix are defined by

$$\dot{p}_{a_n} = \int_0^t \dot{p} e^{-\frac{V}{b}\beta_n(t-\tau)}\, d\tau \qquad 1 \le n \le N_L \qquad \ddot{p}_{a_n} = \dot{p} - \frac{V}{b}\beta_n \dot{p}_{a_n} \tag{39}$$

Equations (38) and (39) can now be combined together to form the state space equations. This can be formulated by transforming these expressions to a first order differential equation with the states and the state space matrix defined as

$$x = \begin{bmatrix} p^T & \dot{p}^T & \dot{p}_{a_1}^T & \dot{p}_{a_2}^T & \cdots & \dot{p}_{a_{N_L}}^T \end{bmatrix}^T$$
$$\dot{x} = [A_s]\{x\} + \{b\} \tag{40}$$

where the state matrix of A_s is:

$$A_s = \begin{bmatrix} 0 & I & 0 & 0 & 0 & 0 \\ -\widetilde{\boldsymbol{A}}^{-1}\widetilde{\boldsymbol{E}} & -\widetilde{\boldsymbol{A}}^{-1}\widetilde{\boldsymbol{D}} & \widetilde{\boldsymbol{A}}^{-1}A_3 & \dots & \dots & \widetilde{\boldsymbol{A}}^{-1}A_{N_L+2} \\ 0 & I & -\frac{V}{b}\beta_1 I & 0 & \dots & 0 \\ 0 & I & 0 & -\frac{V}{b}\beta_2 I & \ddots & \vdots \\ \vdots & \vdots & \vdots & \ddots & \ddots & 0 \\ 0 & I & 0 & \dots & 0 & -\frac{V}{b}\beta_{N_L} I \end{bmatrix} \tag{41}$$

and the geometric nonlinear force vector is expressed as

$$\{b\} = \begin{Bmatrix} 0 \\ -A^{-1}\boldsymbol{E}_{\boldsymbol{NL}}(P) \\ 0 \\ 0 \\ \vdots \\ 0 \end{Bmatrix} \tag{42}$$

Therefore, the state space formulation can now be solved using the time domain integration in order to calculate the response for any given input force such as initial deflection, initial velocity or gust.

3 Simulation model

The Patil and Hodges wing model [4, 5, 16] has been considered, in this study. The properties of the wing are shown in table (1) [4, 5, and 16]. The finite element software i.e MSC NASTRAN is used to model the wing which includes the structural information calculated from the finite element grid and the aerodynamic information is obtained using the doublet lattice method. Figure (6) shows the finite element representation of structural and aerodynamic grid. For a simplification of the analysis, the wing is modelled as a beam using CBEAM elements, and a fully clamped boundary condition is defined at one end of the beam. A mesh convergence study was made to determine the appropriate number of elements to be included in the model in order to give a reasonable accuracy to the overall solution. As a result, the element density of 36 elements along the beam has been chosen.

The normal mode analysis (sol 103) was first performed using MSC NASTRAN to obtain the eigensolutions of the model; and the mass and stiffness matrices both in physical and modal coordinates can also be determined. The first three bending modes are found at 0.36Hz, 2.23Hz and 6.22Hz and the first torsion mode is 6.0657Hz. Having defined the nonlinear static test cases, the finite element nonlinear static analysis is performed under sol 106 of MSC NASTRAN to obtain the resultant displacement for each of the defined load cases.

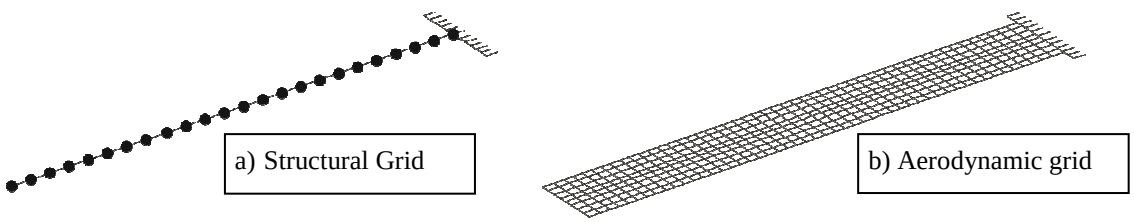

Figure (6) : structural and aerodynamic grids for the HALE wing

Flutter analysis was then carried out to predict the flutter speed of the considered model at the given flight condition by using the P-K method. At the same time, the complex AIC modal matrices are extracted from this analysis by using the DMAP as this information will later be used for the approximation of the generalised aerodynamic in term of RFA.

Half span (S)	16m
Chord (c)	1m
Mass per unit length	0.75 kg/m
Spanwise elastic axis	50 percent chord
Center of gravity	50 percent chord
Bending rigidity	2×10^4 Nm^2
Torsional rigidity	1×10^4 Nm^2
Flight condition Altitude Air Density	 20km 0.0889 kg/m^3

Table 1: Patil-Hodges wing data [4,5,16]

4 Results

Nonlinear stiffness coefficients were obtained using the combined modal/FE approach. In order to observe the accuracy of the NLROMM, a comparison has been made with FEA (nonlinear static) based on the predefined nonlinear static test cases. Table (2) shows the best fit solution of the nonlinear stiffness coefficients which are to be considered for the dynamic aeroelastic analysis, while figure (7) and (8) show the comparison between the NLROMM and FE-nonlinear static analysis. It can be seen from these figures that a very good agreement has been achieved for this modal model. Therefore, having defined the geometric nonlinearity of the wing, it is now possible to couple the structure with the aerodynamic forces in order to simulate the aeroelastic analysis.

Reduction of the number of polynomial terms is essential especially when the dynamic aeroelastic response is considered. If too many cross-coupling terms (nonlinear coefficient) are included in the system, the time response numerical integrator may fail to convergence.

Nonlinear Stiffness coefficient – AEROELASTIC ANALYSIS							
mode 1		*mode 2*		*mode 3*		*mode 4*	
$p_1p_4^2$	6.425	$p_2p_4^2$	50.72	p_3^3	1572	$p_1^2p_4$	15.67
$p_2p_1^2$	-0.5508	$p_1p_2^2$	-7.749			$p_1*p_4^2$	-109.5
$p_1^2p_4$	-0.7499	$p_1^2p_2$	-3.609			p_4^3	196.3

Table 2: nonlinear stiffness coefficient to be considered for aeroelastic analysis
(p_1, p_2, p_4 are bending modal coordinates, whilst p_3 refers to the torsional modal coordinate)

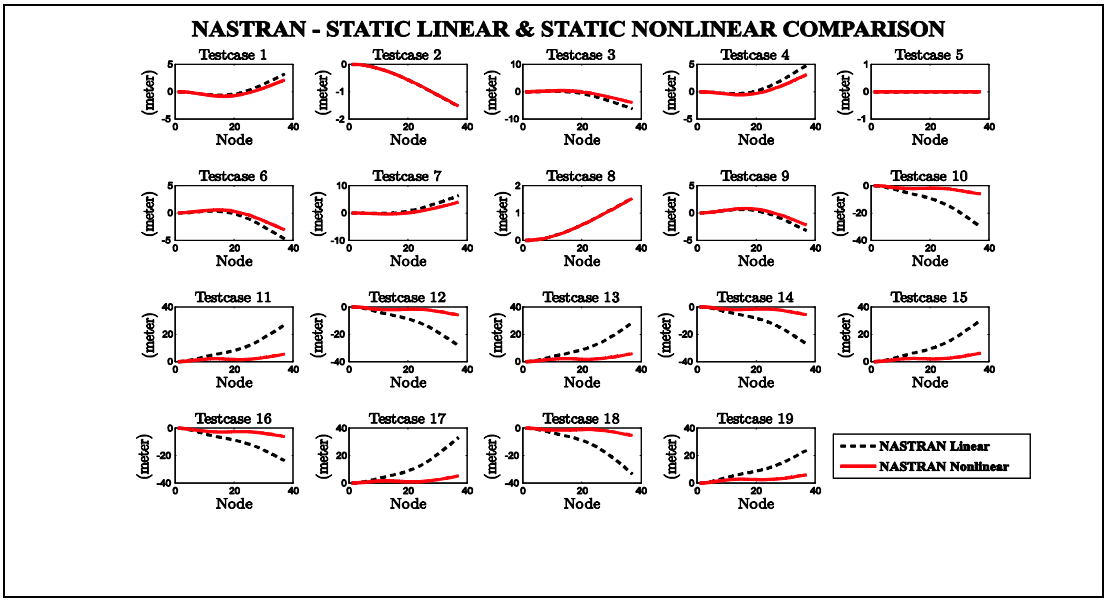

Figure (7) : Comparison between the NLROMM and FE-nonlinear static analysis in bending

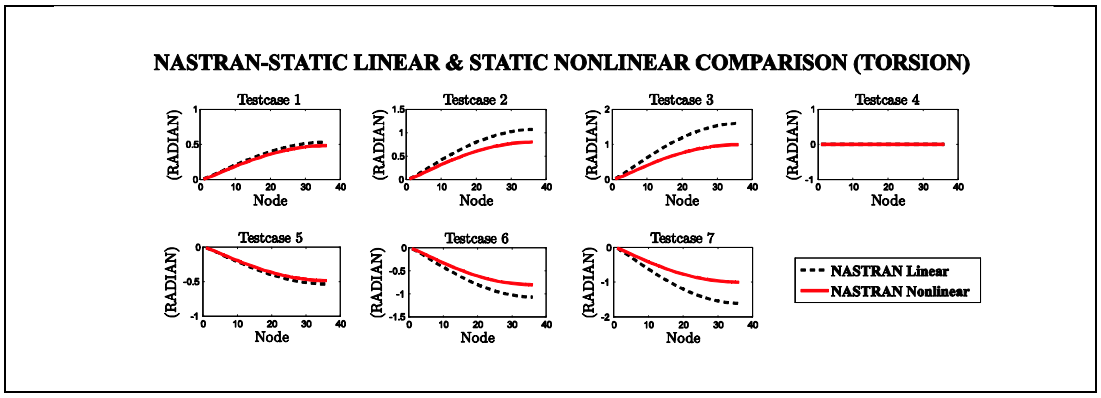

Figure (8) : Comparison between the NLROMM and FE-nonlinear static analysis in torsion

Linear flutter analysis was carried out in order to determine the linear aeroelastic behaviour of the model under investigation for a range of air speeds at the given flight condition. By solving the eigenvalue problem of the linear aeroelastic dynamic system, the flutter and divergence instabilities can be determined by investigating on the calculated data in graphical representation of V-g and V-ω diagrams.

The V-g and V- ω diagrams of the wing model using the MAST are shown in figure (9). From the figure, the flutter speed is found at 23.35m/s by the first crossing of one of the mode from positive to negative of the damping ratio. While Figure (10) shows the V-g and V-w diagrams of the wing model using the DLM which is calculated using the p-k method of MSC NASTRAN. The linear flutter speed of this aeroelastic model can be found at 35.25m/s with a corresponding flutter frequency of 4.123Hz when one of the damping ratio becomes zero. This gives close agreement with the flutter result in ref [16].

There is a huge difference between the aeroelastic models that using the MAST (Quasi-unsteady aerodynamics) and DLM (frequency dependent -unsteady aerodynamics) in terms of linear flutter speed results. This is to be expected as the MAST does not accurately model the frequency dependency and a constant of $\mathbf{M}_{\acute{o}}$ term is used to define the unsteady behaviour of the aerodynamics. Therefore the effect of frequency dependent on aerodynamics cannot be neglected and needs to be accounted for.

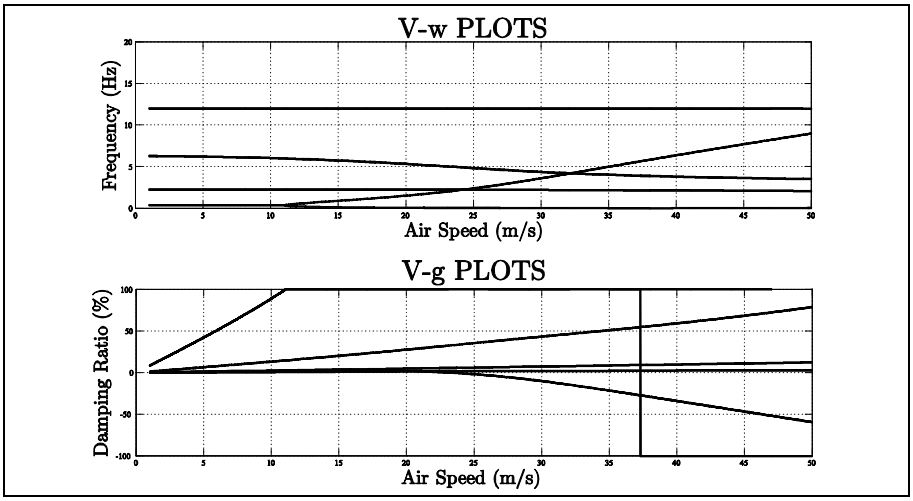

Figure (9) : Frequency and Damping trends for the HALE model
Aerodynamic model – modified unsteady aerodynamic strip theory
Flutter speed = 23.35 m/s

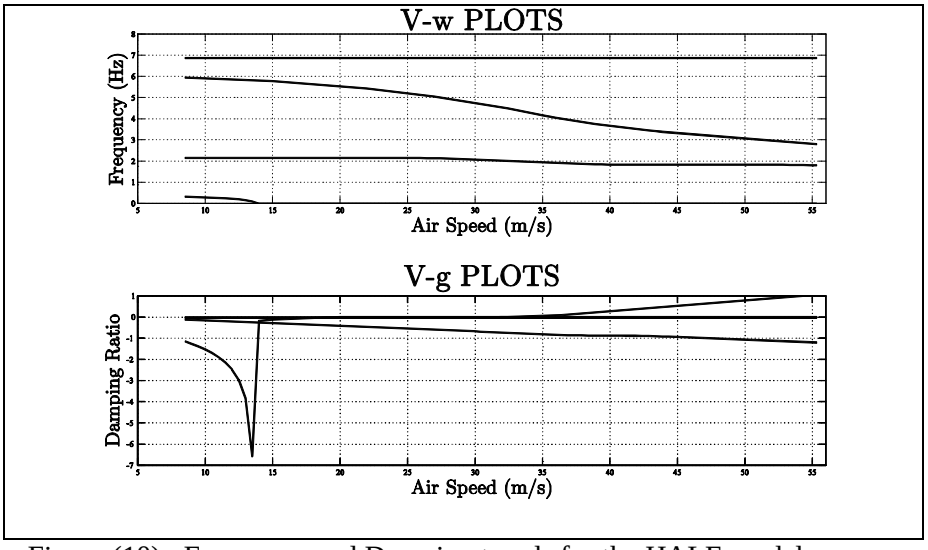

Figure (10) : Frequency and Damping trends for the HALE model
Aerodynamic model – DLM
Flutter speed = 35.25 m/s, Flutter Frequency = 4.123 Hz

Figure (11) and (12) shows the time history of the tip deflection and tip twist at flight speeds just slightly above the linear flutter speed. From the figure, it is clearly shown that the amplitudes of the oscillations increase until a limit cycle oscillations (LCO) is encountered. It occurs due to the changes in the behaviour of the structural stiffness, where in this case, the structural stiffness is increases as the deflection get larger, hence limiting the motion of the system. If a structure with a linear stiffness is considered, the motion will grow exponentially with time to infinity when the critical speed is exceeded (in practice, failure due to flutter will occur). Therefore, the wing is required to deflect until the nonlinear hardening stiffness, either on bending or torsion, takes place to limit the oscillations. This explains the limit cycle motion as shown in figure (11) and (12). Figure (13) shows a steady state LCO amplitude predicted for the wing model with the inclusion of structural nonlinearities. Above the linear flutter speed, LCO form and the amplitude will grows as the speed increases beyond critical speed. Note the very high twist values which will require more accurate modelling of the stall behaviour.

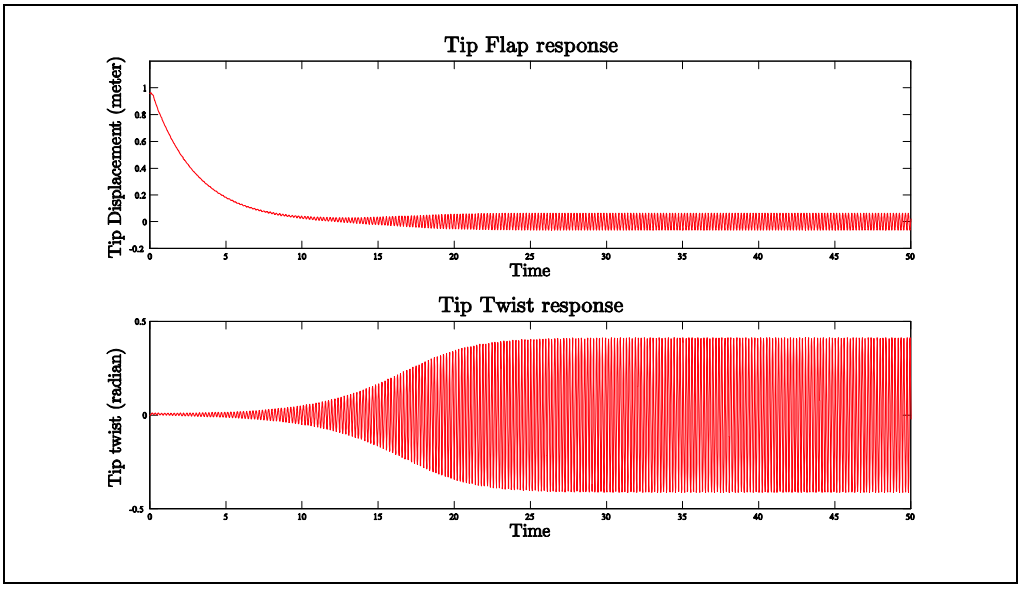

Figure (11) : Time history for flapwise and tip twist deflection
Velocity = 25m/s, Angle of attack = 0^o
Aerodynamic model – Modified Aerodynamic Strip Theory

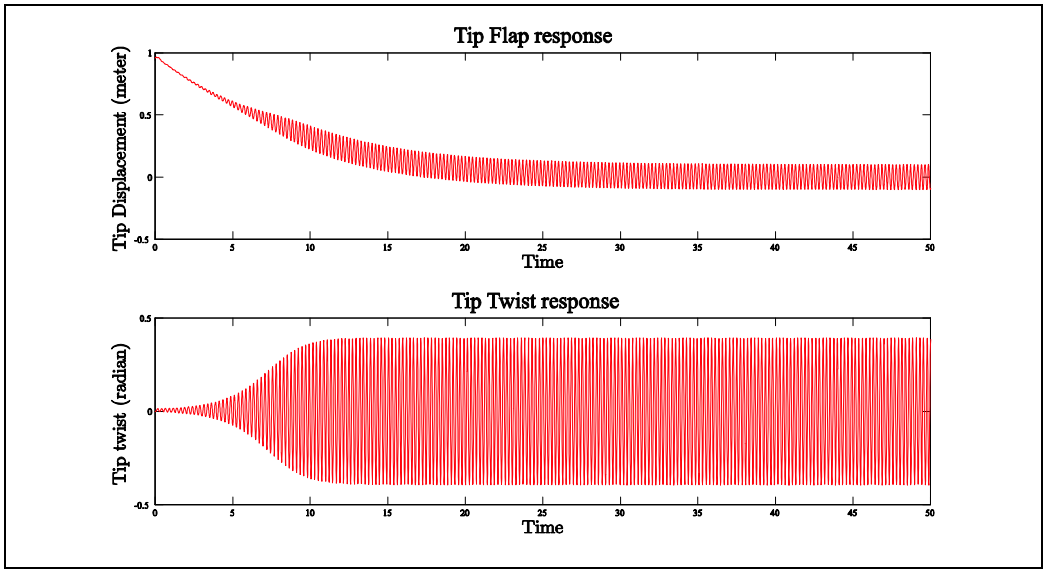

Figure (12) : Time history for flapwise and tip twist deflection
Velocity = 37m/s, Angle of attack = 0^o
Aerodynamic model – RFA of DLM

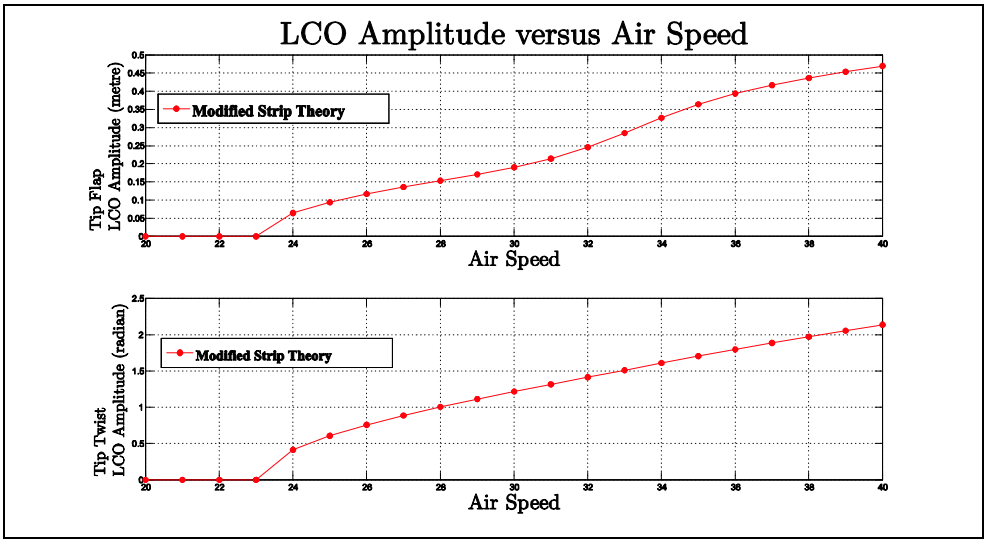

(a)

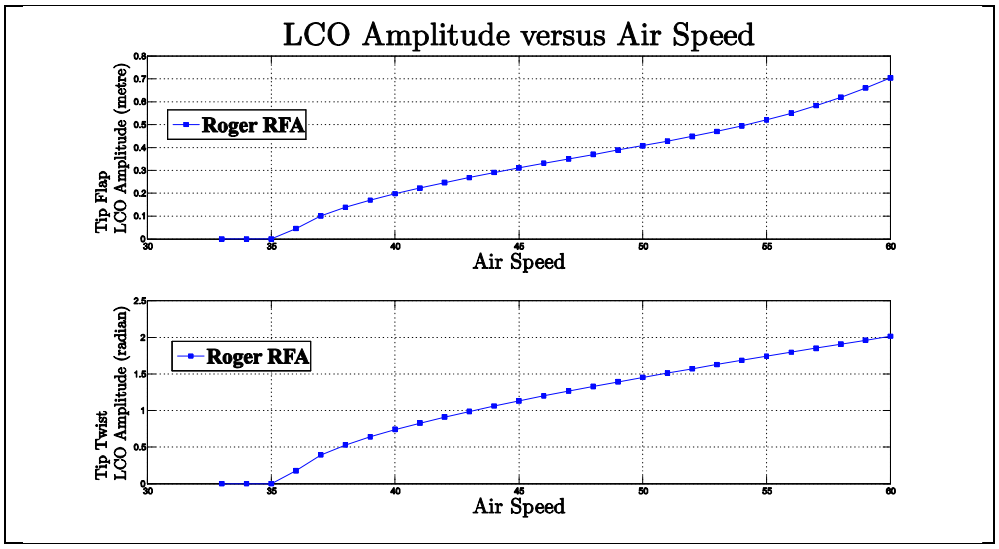

(b)

Figure 13 : LCO amplitude of tip flap and tip twist

5 Conclusions

In this paper, a geometric nonlinear modal model of the wing is developed based on the combined modal/FE approach. Very good agreement between the NLROMM and FE nonlinear static analysis has been obtained. Dynamic aeroelastic responses have been simulated using the NLROMM and including DLM. The effect of the geometric nonlinearities was investigated and there can be significant changes in the aeroelastic behaviour due to the large deflections under the aerodynamic load compared to a linear model.

Further work is required to include the cross couplings between bending and torsional geometric nonlinearities, stall characteristics of the wing, inclusion of the nonlinear couplings between the edge-wise bending and torsion and implementation of a nonlinear stability analysis.

Acknowledgement

The authors wish to thank to the Malaysian Ministry of Higher Education (MOHE) and the Universiti Putra Malaysia (UPM) for their support of M. Y. Harmin in this work. They are grateful for the input of Dr. Gareth Vio and Hamed Haddad Khodaparast from the Dynamics & Control Group of the University of Liverpool for useful discussions and assistance.

References

[1] Noll TE, Brown JM, Perez-Davis ME, Ishmael SD, Tiffany GC, Gaier M, *Investigation of the Helios Prototype Aircraft Mishap,* NASA Technical report (2004)..

[2] Palacios R, Cesnik CES, Reichenbach EY, *Re-examined Structural Design Procedures for VeryFlexible Aircraft,* 2007 International Forum of Aeroelasticity and Structural Dynamics, Stockholm, Sweden.

[3] Palacios R & Cesnik CES *Structural Models for Flight Dynamic Analysis of Very Flexible Aircraft,* –50th SDM2009.

[4] Patil, M J; Hodges, D H, *On the importance of aerodynamic and structural geometrical non-linearities in aeroelastic behavior of high-aspect-ratio wings*. Journal of Fluids and Structures. Vol. 19, no. 7, pp. 905-915.Aug. 2004

[5] Patil MJ, Hodges DH, Cesnik CES, *Non-linear Aeroelastic Analysis of Complete Aircraft in Subsonic Flow,* (2000) Journal of Aircraft 37 (5), pp. 753-760 .

[6] Shearer CM, Cesnik CES (2007). *Non-linear Flight Dynamics of Very Flexible Aircraft,* Journal of Aircraft 44 (5) pp. 1528-1545.

[7] Cesnik CES, Su W., *Non-linear Aeroelastic Modeling and Analysis of Fully Flexible Aircraft,* (2005) AIAA Paper No. 2005-2169.

[8] Z. Wang et al, *Time Domain Non-linear Aeroelastic Analysis for HALE Wings,* 47th SDM 2006

[9] McEwan, M I; Wright, J R; Cooper, J E; Leung, A Y T , *A combined modal/finite element analysis techniquefor the dynamic response of a non-linear beam to harmonic excitation,* Journal of Sound and Vibration. Vol. 243,no. 4, pp. 601-624. 14 June 2001.

[10] McEwan, M I; Wright, J R; Cooper, J E; Leung, A Y T , *A finite element/modal technique for non-linearplate and stiffened panel response prediction,* 42nd AIAA SDM Conference. 2001.

[11] Radu, A., Yang, B., Kim, K., and Mignolet, M.P., *Prediction of the Dynamic Response and Fatigue Life of Panels Subjected to Thermo-Acoustic Loading*, 45th AIAA/ASME/ASCE AHS/ ASC Structures, Structural Dynamics, and Materials Conference. 2004. Palm Springs, CA.AIAA 2004-1557

[12] Muravyov, A.A., and Rizzi, S.A., *Determination of Non-linear Stiffness with Application to RandomVibration of Geometrically Non-linear Structures*, Journal of Computers and Structures, 2003. 81(15): p. 1513-1523.

[13] Hollkamp JJ. et al. *The Non-linear Response of a Plate to Acoustic Loading: Predictions and*

Experiments, 47th AIAA/ASME/ASCE/AHS/ASC Structures, Structural Dynamics, and Materials Conference 2006

[14] Liu DD. et al *Non-linear Aeroelastic Methodology for a Membrane-on-Ballute Model with Hypersonic BowShock*, 50th SDM. AIAA-2009-2363

[15] Scott, R.C., Bartels, R. E., and Kandil, O. A. *An Aeroelastic Analysis of a Thin Flexible Membrane*, 48th AIAA/ASME/AHS/ASC Structures, Structural Dynamics, and Materials Conference. 2007.AIAA 2007-2316

[16] Patil, Mayuresh J. (Georgia Inst of Technology, Atlanta, United States); Hodges, Dewey H.; Cesnik, Carlos E.S. *Limit cycle oscillations in high-aspect-ratio wings*, Collection of Technical Papers - AIAA/ASME/ASCE/AHS/ASC Structures, Structural Dynamics and Materials Conference, v 3, p 2184-2194, 1999

[17] Wright J.R and Cooper, J.E. *Introduction to Aircraft Aeroelasticity and Loads*, 2007 John Wiley

[18] Roger, K.L., *Airplane Math Modelling Methods for Active Control Design*, AGARD, Rept. AGARD-CP-228,1977

[19] Dimitriadis, G., *Bifurcation Analysis of Aircraft with Structural Nonlinearity and Freeplay Using Numerical Continuation*, Journal of Aircraft 45 (3), pp. 893-905.

[20] "ZAERO Ver. 7.2 *Theoretical Manual*, Zona Technology, Scottsdale, AZ, 2004.